ELSEVIER

Contents lists available at ScienceDirect

Journal of Environmental Chemical Engineering

journal homepage: www.elsevier.com/locate/jece



Chip-scale mercury-free UV light sources enabling Log-9 reduction of E. coli

Vijay Kumar Sharma ^{a,b,*}, Kelyn Seow ^c, Patricia Conway ^{c,d}, Emma Eriksson ^e, Jonas Tirén ^e, Hilmi Volkan Demir ^{a,b,*}

- ^a LUMINOUS! Center of Excellence for Semiconductor Lighting and Displays, School of Electrical and Electronic Engineering, School of Physical and Mathematical Sciences, School of Materials Science and Engineering, Nanyang Technological University, Singapore 639798, Singapore
- ^b UNAM-National Nanotechnology Research Center and Institute of Materials Science and Nanotechnology, Department of Electrical and Electronics Engineering, Department of Physics, Bilkent University, Ankara 06800, Turkey
- c Singapore Centre for Environmental Life Sciences Engineering (SCELSE), Nanyang Technological University, Singapore 637551, Singapore
- d School of Biological, Earth and Environmental Sciences, The University of New South Wales, Sydney 2052, Australia
- ^e PureFize Technologies AB, Uppsala Business Park, Virdings Allé 32B, Uppsala 754 50, Sweden

ARTICLEINFO

Keywords: UV disinfection Log-9 reduction E. coli Mercury-free UV light chips

ABSTRACT

Escherichia coli (E. coli) contamination remains a critical threat to food safety, healthcare, and water treatment sectors, demanding highly effective and scalable disinfection solutions. This study demonstrates 9-log reduction of E. coli using a compact, mercury-free UV light chip that emits a broad spectrum (250–350 nm) with peak intensity at 262 nm, directly targeting the DNA absorption maximum. The device achieves this high level of microbial inactivation at a dose of approximately 45 mJ/cm² by simultaneous activation of multiple germicidal pathways—direct DNA damage near 265 nm, protein oxidation and membrane disruption in the 280–300 nm region, and oxidative stress—driven mechanisms between 300–350 nm. Unlike traditional chemical disinfectants and costly UV systems, this solid-state, free-electron driven, chip-scale device offers a safer, more energy-efficient, and highly scalable alternative. These findings set a new standard in UV disinfection performance and pave the way for advanced microbial control across critical industrial and environmental applications.

1. Introduction

Escherichia coli (E. coli) is a bacterium that is commonly found in the gut of humans and warm-blooded animals. [1] Its presence has significant implications across various critical industries, including healthcare, water distribution, food processing, industrial manufacturing, marine industries, and sanitation. [2] In the food and beverage sector, E. coli contamination can lead to serious foodborne illnesses, necessitate product recalls, and invite regulatory scrutiny, thereby impacting consumer safety and business operations. [3] In healthcare settings, E. coli infections present challenges that increase healthcare costs and complicate patient care. [4] Similarly, E. coli contamination in other industries poses health risks, driving the need for stringent hygiene and testing protocols. Addressing E. coli contamination across these sectors requires comprehensive sanitation practices and adherence to safety regulations to mitigate health risks and ensure product safety.

Most traditional methods to control *E. coli* contamination, such as chemical disinfectants and heat treatments, have notable limitations.

[5] Chemical disinfectants like sodium hypochlorite can achieve up to a 6-log reduction (99.9999 %) in microbial populations but often leave behind chemical residues, which can be problematic. [5] Heat treatments, such as pasteurization and autoclaving, are highly effective; pasteurization generally achieves a 5-log reduction, while autoclaving can result in complete sterilization. [6] However, these methods may not be suitable for heat- or moist-sensitive materials and can require substantial energy input. Advanced disinfection techniques, such as electron-beam irradiation, have shown promise by achieving significant log reductions without the need for high temperatures or chemical residues. [7] Despite their effectiveness, these techniques are often complex and expensive, limiting their practicality for widespread use.

Among various disinfection methods, UV irradiation, when used with proper safety measures, is particularly effective at achieving significant log reductions in a wide range of viruses, bacteria, and fungi. [8–10] The germicidal efficacy of UV light primarily stems from the UVC spectrum (200–280 nm), which induces significant molecular damage to nucleic acids, leading to cell death through mechanisms such as

^{*} Corresponding authors at: LUMINOUS! Center of Excellence for Semiconductor Lighting and Displays, School of Electrical and Electronic Engineering, School of Physical and Mathematical Sciences, School of Materials Science and Engineering, Nanyang Technological University, Singapore 639798, Singapore E-mail addresses: vksharma@ntu.edu.sg (V.K. Sharma), hvdemir@ntu.edu.sg (H.V. Demir).

cyclobutane-pyrimidine dimer formation and other DNA lesions. [11, 12] Contributing to the germicidal efficacy is also light from the UVB spectrum (280-315 nm) which has a significant impact on proteins by generation of reactive oxygen species (ROS). [13] However, conventional UV disinfection methods often rely on 254 nm mercury lamps, which pose environmental and health risks due to mercury toxicity, driving increased demand for safer alternatives in line with the Minamata Convention on Mercury's efforts to reduce global mercury emissions. [14,15] AlGaN-based UV light-emitting diodes (LEDs) are emerging as viable replacements for mercury lamps due to their ability to be tuned across the UV spectrum (210-355 nm) by alloying GaN with AlN materials. [16,17] Despite their promising potential, the performance of AlGaN-based UVC LEDs is currently hindered by factors such as high dislocation densities, low hole concentrations, and poor light extraction efficiency. [18-20] Among these issues, thermal management is particularly critical for UVC LEDs, as devices operating near 260 nm require high Al fractions ($Al_xGa_{1-x}N$, x > 0.5), which inherently reduce efficiency and exacerbate heat-related degradation. Junction heating accelerates external quantum efficiency droop and can cause radiant flux losses exceeding 50 % within only a few hundred hours when insufficient cooling is provided. Therefore, effective heat management is essential to ensure optimal UVC LEDs performance and longevity. [21] While electron-beam (e-beam) pumped semiconductor light sources have shown notable improvements in power output and efficiency, they remain commercially impractical because their reliance on thermal electron guns and ultra-high vacuum (~10⁻⁷-10⁻⁸ mbar) necessitates bulky chambers, pumps, and feedthroughs that greatly increase size, complexity, and cost. [22,23]

In this work, we introduce a novel class of compact, chip-scale, free-electron driven broadband ultraviolet (UV) light sources that deliver high efficiency while overcoming the limitations of existing disinfection technologies through a completely mercury-free design. We achieved a 9-log reduction in E. coli with a dosage of $\sim\!45~\rm mJ/cm^2$, highlighting the strong potential of this approach for advanced microbial inactivation. As shown in Fig. 1, the advanced version of our previous chip, presented in our earlier work, [24] features a fully packaged UV chip (27 mm diameter, 4 mm thick) with a UVC phosphor anode and a ZnO nanorod (NR) cathode. Leveraging on-chip cathodoluminescence and field-emission technology, our UV chips offer remarkable reliability, instant ON/OFF capability, extended operational lifetimes, and low-temperature tolerance, along with complete design flexibility.

These exceptional features position our UV chips as highly suitable for a wide array of applications, providing a safe, effective, and sustainable solution for microbial inactivation.

2. Experimental section

2.1. Bacterial cultivation

The germicidal experiment was conducted using *E. coli* (ATCC 25922), cultivated with standard microbiological techniques. Overnight cultures of *E. coli* were prepared by transferring a single colony from a glycerol-streaked Tryptic Soy Agar (TSA, BD DifcoTM) plate to 5 mL Tryptic Soy Broth (TSB, BD DifcoTM) and incubating in a shaking incubator at 37 °C with a shaking speed of 200 rpm. Aliquots (1 mL) of overnight cultures were washed with 9 mL of fresh sterile TSB, centrifuged to collect the pellet, and then the pellet was washed twice with sterile PBS. The washed pellet was resuspended to yield a stock concentration of 10^{10} CFU/mL using optical density and a standard curve. The stock cultures were serially diluted in 10-fold steps up to 10^{-10} . Aliquots ($100~\mu$ L) of each dilution were spread on the TSA agar plates immediately prior to use in the germicidal experiments.

2.2. Experimental setup

The experimental setup for germicidal testing (Fig. 2) was conducted within a biosafety cabinet (BSC) equipped with precise temperature and humidity controls. In this controlled environment, the UV chip was strategically positioned at a fixed distance of 5 cm from the base on which the Petri dishes containing microbial inoculants were carefully placed. Control inoculated plates were also included but not subjected to exposure. The UV chip operated consistently at a stable electrical input of 500 mW (\sim 6–7 kV, 70–85 μ A) ensuring uniform exposure. Prior to initiating the experiment, the BSC was thoroughly sanitized with 70 % ethanol and subjected to a 30-minute UVC treatment to eliminate any potential contaminants. Every item within the cabinet was meticulously cleaned to maintain a contamination-free environment, with the temperature held consistently close to 28°C and the humidity maintained at approximately 55 %. This rigorous preparation ensured the reliability and accuracy of the germicidal testing.

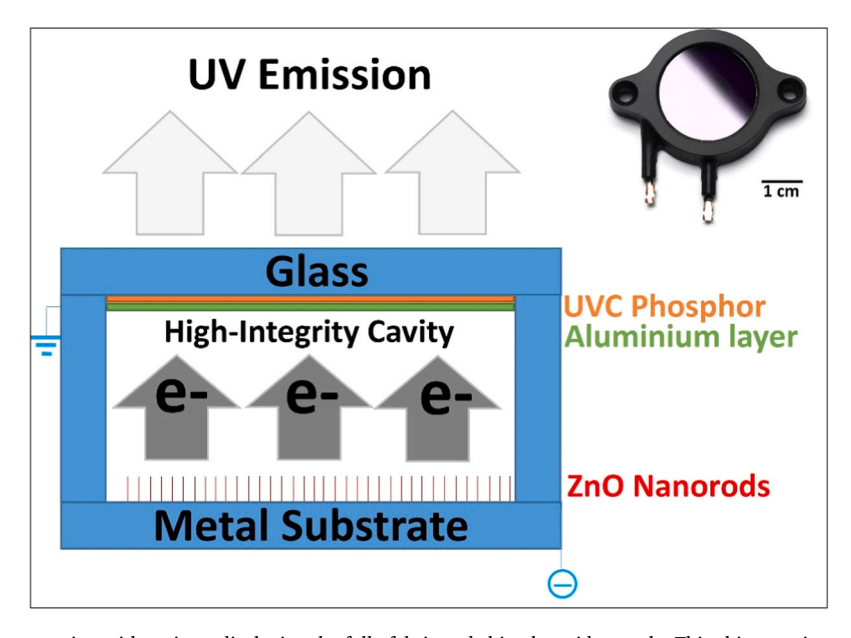


Fig. 1. UV Chip: Schematic representation with an inset displaying the fully fabricated chip alongside a scale. This chip constitutes a substantial advancement over our previously published work. [24].

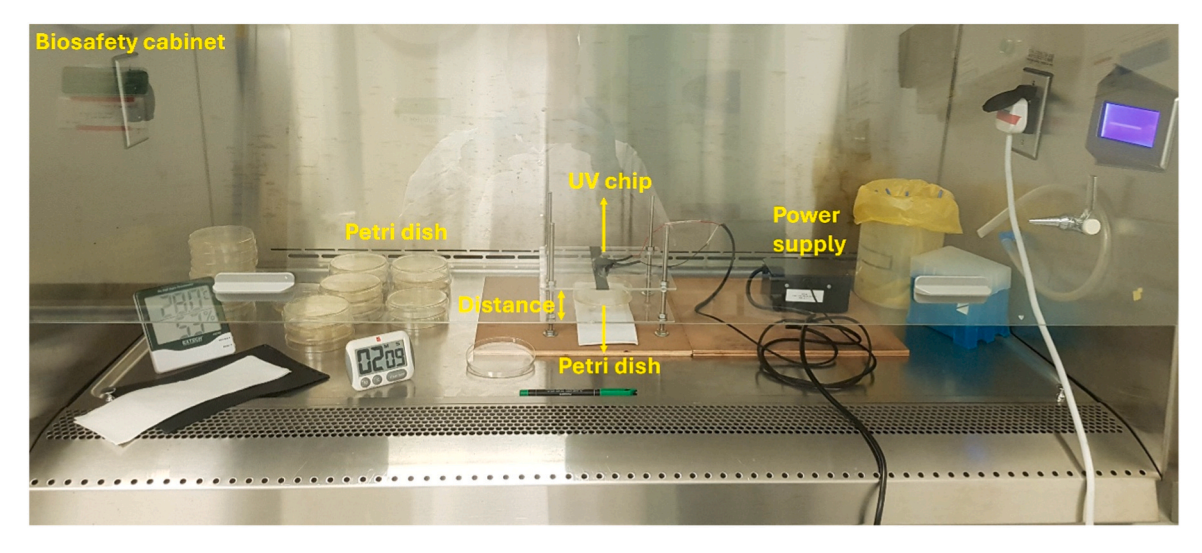


Fig. 2. Germicidal Setup: Experimental configuration for germicidal testing.

2.3. Photometric analysis

Photometric characterization of the UV chips was performed using a spectrophotometer (AvaSpec-2048L, Avantes) in conjunction with an integrating sphere (THORLABS 4P3). The THORLABS integrating sphere enabled accurate measurement of the total power output, with most chips exhibiting a radiant flux of $\sim\!10$ mW at 500 mW input. To evaluate the radiation pattern, a custom-designed setup was employed, providing detailed insights into the angular distribution of UV emission. The UVC intensity emitted by the UV chips was measured with an ILT2400 handheld light meter, calibrated at 270 nm. The UVC intensity was measured in mW/cm² both before and after the germicidal experiments, providing a dependable assessment of the UVC dosage necessary for achieving germicidal activity.

2.4. Germicidal experiments

In the experimental setup, a single UV chip operating at an input power of 500 mW was strategically positioned above a Petri dish with the E. coli as described above. E. coli samples with precisely calibrated concentrations, ranging from 10^6 to 10^{10} colony-forming units (CFUs), were exposed to the UV chip for intervals of 60, 120, 180, 240, 300, 360, 420, 480, 540, and 600 s. Control samples of each concentration were not exposed to the UV light. After irradiation, the test and control plates of E. coli bacteria were incubated for 18 h at 37° C to evaluate the effects of the exposure.

2.5. Inactivation model

The inactivation curves of *E. coli*, evaluated during UV chip treatments, were analysed using a linear empirical model (Eq. 1) to determine the pseudo-first-order UV inactivation rate constant (k) for each UV dose (D). In this model, N_s represents the density of surviving bacteria, while N_0 denotes the initial bacterial concentration, of the inoculum spread on the plates:

$$Log \ inactivation \ = \ log_{10} \left(\frac{N_0}{N_s} \right) = \ \textit{kD} \eqno(1)$$

The results represent the viable *E. coli* cells presented as mean Colony Forming Units (CFU) per test. For each UV dose, at least five replicates were used for each concentration of *E. coli*.

2.6. Simulations methodology

We employed COMSOL Multiphysics with the Ray Optics Module to evaluate the irradiance power distribution (W/m^2) on the Petri dish surface as a function of the distance between the Petri dish and the UV chip. The optimal separation was determined by varying the chip-to-dish distance and identifying the point at which the irradiance provided the maximum and most uniform surface coverage. The simulations accounted for both the spectral weighting and the angular emission characteristics of the UVC chip to ensure accurate representation of dose delivery.

3. Results and discussion

3.1. UV chips optical properties

The operating principle of our UV chips marks a substantial leap forward from conventional technologies, utilizing advanced cathodoluminescence within a high-integrity vacuum cavity to achieve efficient field emission. These chips employ high-quality ZnO nanorods as a cold cathode, where high voltage and minimal current create an intense electric field at the nanorod tips, liberating electrons that are then accelerated through the vacuum towards an anode coated with UVC phosphor. For this work, we have used Lu₂Si₂O₇:Pr³⁺ as the phosphor due to its ability to produce a broadband UV emission under electron excitation. This interaction generates broad emission spectra of UV light from our UV chips, as illustrated in Fig. 3a, highlighting UVA, UVB, and UVC components with a peak intensity at 262 nm, known for its optimal biocidal effectiveness.

Selecting the appropriate UVC wavelength and the spectral overlap is crucial for effective microbial inactivation, with light in the 260–265 nm range being particularly effective at disrupting the DNA and RNA of bacteria, viruses, and fungi, thereby preventing replication, and inducing cell death. This effectiveness is demonstrated by 70 % spectral overlap between the typical *E. coli* deactivation curve and the emission spectra of our UV chips (see Fig. 3a). Additionally, optimizing the radiation pattern is vital for achieving uniform disinfection. As shown in Fig. 3b, the radiation pattern of our UV chips peaks perpendicular to the junction plane and diminishes according to the cosine of the angle from this axis, with intensity dropping to 50 % at approximately 60 degrees. This precisely controlled light distribution ensures both broad and focused coverage, facilitating thorough disinfection while preventing underexposed areas, thus ensuring consistent, high-quality performance. Unlike conventional UVC LEDs, our chips require no external

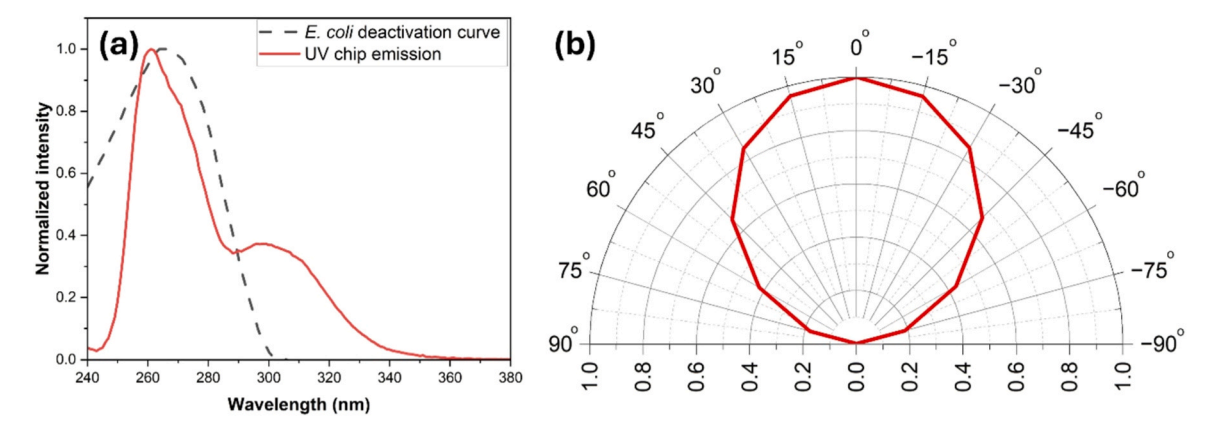


Fig. 3. Optical Properties: (a) Emission spectrum of the UV chips showing its overlap with the typical *E. coli* deactivation curve, and (b) radiation pattern of the UV chips.

thermal management because they operate at relatively low input power (5–6 kV, $\sim\!85{-}100~\mu\text{A})$ and rely on cold field-emission cathodes, which inherently minimize internal heating. This design addresses one of the key limitations of UVC LEDs, where heat buildup accelerates performance degradation and shortens device lifetime. Moreover, our UV chips demonstrated stable and consistent output across a broad temperature range (–20 °C to 80 °C; Figure S1, SI), further underscoring their robustness. Finally, while UVC LEDs typically emit highly directional light, our chips exhibit a broader emission pattern, enabling superior area coverage and enhanced disinfection efficiency.

3.2. UV setup optimization

In addition to the pivotal role of wavelength and radiation pattern, irradiance and the precise distance between the UV source and target are also integral to maximizing UV light effectiveness for disinfection. We rigorously evaluated these parameters by measuring irradiance to determine the optimal separation between the UV chip and the Petri dish containing $\it E.~coli$ bacteria. Using a hand-held light meter (ILT 2400) calibrated to 270 nm, we recorded incident irradiance in mW/cm² with the sensor positioned parallel to the UV chip at distances ranging from 1 cm to 12 cm.

The data, depicted in Fig. 4a, align with the inverse square law, showing a clear reduction in light intensity as distance increases. Our findings establish that a 5 cm distance between the UV chip and the Petri dish is optimal, balancing the chip's function as a point source with the

dish's role as a surface target. This distance ensures maximal irradiation and uniform exposure, while distances beyond 5 cm led to diminished intensity and prolonged exposure times, and shorter distances cause significant intensity variations across the Petri dish. Fig. 4b illustrates the intensity gradient from center to edge of the Petri dish, with the inset displaying the simulated light distribution at the 5 cm distance. This precise calibration ensures measurable uniformity across the test surface, providing a robust framework for effective UV disinfection.

3.3. UV dosage optimization

The effectiveness of UV light disinfection is linked to the precise dosage of UV energy delivered over time. The precise dosage, defined as the product of UV light intensity (in mW/cm²) and exposure time (in seconds), is fundamental to achieving optimal microbial inactivation. In this study, we stringently controlled the UV light intensity while systematically varying exposure times to deliver UV doses ranging from 0 to 75 mJ/cm² to the agar plate surface, as detailed in Fig. 5. We employed a standard laboratory timer to measure exposure times from 0 to 600 s, ensuring rigorous control and accuracy. Throughout these experiments, light intensity was continuously monitored to maintain consistency. A comprehensive set of exposure times (60, 120, 180, 240, 300, 360, 420, 480, 540, and 600 s) was evaluated at a distance of 5 cm from the light source to determine the doses required for significant bacterial load reductions.

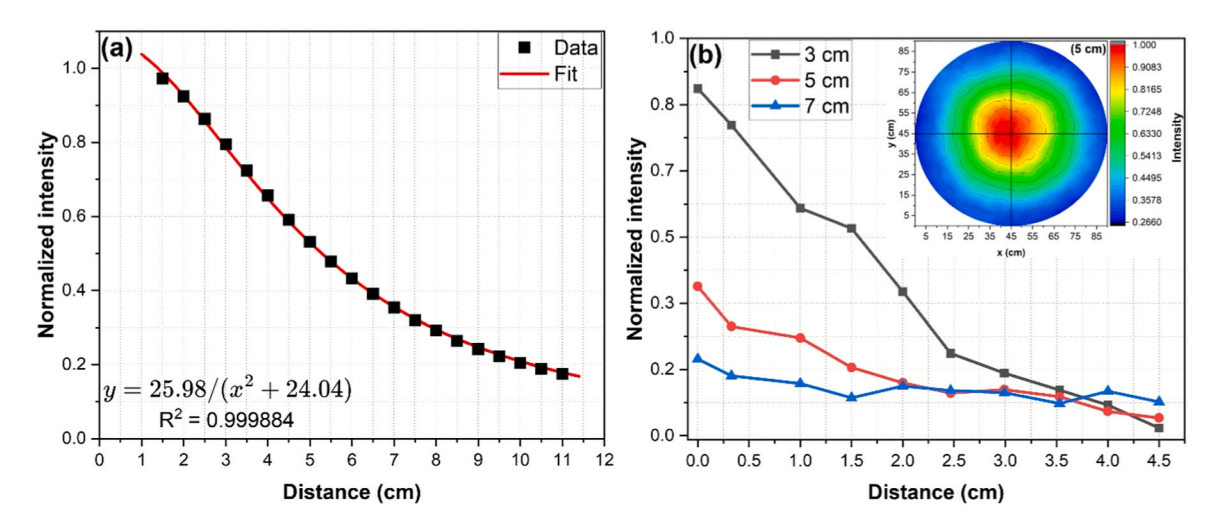


Fig. 4. Irradiance Measurements: (a) Intensity variation with distance between the light meter and the chip follows an inverse square law. (b) UV irradiance intensity changes from the center to the edge of the Petri dish, with inset showing the simulated UV chip irradiance on the Petri dish at a 5 cm distance.

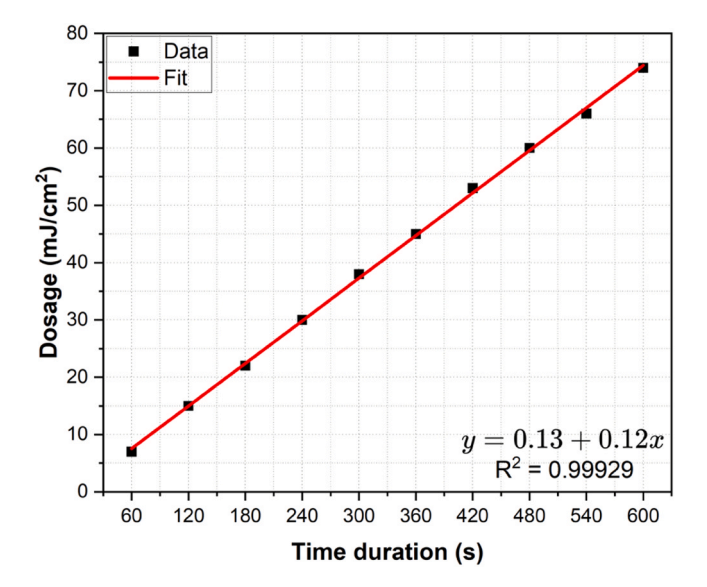


Fig. 5. UV Dosage Measurements: UV dosage increases linearly over time, as shown by the linear fit, with a 5 cm distance between the UV chip and the light meter.

3.4. Germicidal log reduction

Germicidal experiments were conducted to evaluate the efficacy of the UV chips against *E. coli*. The results showed a significant reduction in *E. coli* populations with increasing UV exposure time, achieving a log 9 reduction with a 360-second exposure. For these experiments, we used a single chip with an input power of 500 mW positioned 5 cm from the base of a Petri dish containing *E. coli* bacteria on tryptic soy agar. *E. coli* samples with concentrations ranging from 1000 to 1000,000,000 colony-forming units (CFUs) were irradiated for durations of 60, 120, 180, 240, 300, 360, 420, 480, 540, and 600 s. A control sample, which was not exposed to deep-UV light, was also included. Following irradiation, the *E. coli* inoculated plates were incubated for 18 h at 37°C.

The UV irradiation of E. coli bacteria significantly reduced the viable bacterial populations with increasing exposure times (Fig. 6). Our results demonstrates a log 9 (99.9999999 %) reduction in E. coli with approximately 45 mJ/cm² of UV irradiation (360 s), as presented in Figs. 6 and 7. This performance significantly surpasses our initial results of a log-6 reduction on a different strain of E. coli (ATCC 8739). [24] Literature indicates that various E. coli strains exhibit different log reductions when exposed to UV light. [25] Notably, the ATCC 8739 strain is more resistant to antimicrobial agents than the ATCC 25922 strain used in this study. The key distinction is that ATCC 25922 is widely recognized as the standard quality control strain for antibiotic susceptibility testing due to its consistent behaviour, while ATCC 8739 is primarily used for testing antimicrobial handwashing formulations and media efficacy. [26] Moreover, our UV chips have been further advanced and optimized for increased light output power and uniformity compared to our previous work [24], and the experimental setup has been refined by setting the chip-to-E. coli distance to 5 cm for improved effectiveness. Taken together, the enhanced log reductions reported in this study arise from strain susceptibility, calibrated fluence determination, improved device packaging, and increased experimental rigor, rather than distance optimization alone.

Using a linear empirical model (Eq. 1), the pseudo-first-order UV inactivation rate constant (k) of $\sim 0.12~\text{cm}^2/\text{mJ}$ across different UV doses (D) was calculated, as shown in Fig. 7. These rate constants are consistent with those reported in the literature: for instance, Carabias *et al.* [27] reported a rate of 0.350 cm²/mJ for environmental *E. coli*, while Hijnen *et al.* [28] found a rate of 0.506 cm²/mJ for cultured *E. coli*. The variability in the pseudo-first-order UV inactivation rate constant (*k*) can

be attributed to differences in UV dose, irradiance, the bacterial strain used and environmental conditions, as well as experimental factors such as pathlength, UV wavelength, and equipment calibration, which may explain the discrepancies observed among different studies. Compared to existing disinfection methods, which exhibit considerable variability in efficacy, this study demonstrates consistent and reproducible efficacy. The literature shows that UVC irradiation at 254 nm generally achieves up to a 5-log reduction (99,999 %) in E. coli[29], while chemical disinfectants such as sodium hypochlorite can achieve a 6-log reduction (99.9999 %). [30] Heat treatments, including pasteurization and autoclaving, are also highly effective, with pasteurization reaching a 5-log reduction and autoclaving often resulting in complete sterilization. [6] Advanced methods like electron-beam irradiation have achieved up to a 5.6-log reduction. [7] Additionally, UVC LEDs have been reported to achieve a 2-log reduction at 9.2 mJ/cm² with 10 min of irradiation. [31] A comparative summary of these disinfection methods is provided in Table S1, SI.

Our chip-scale UV light source exhibited high bactericidal activity against E. coli, achieving a log 9 reduction within 6 min, significantly exceeding the performance of conventional disinfection methods. This performance is attributed to the peak wavelength of 262 nm that was used, and 70 % spectra overlap with the typical deactivation curve of E. coli, ensuring peak absorption by microbial DNA. In contrast to mercury lamps that operate at a fixed 254 nm and UVC LEDs emitting at discreet wavelengths ranging from 260 to 350 nm, our UV chip emits broadly across 250-350 nm, enabling simultaneous activation of multiple germicidal mechanisms-direct DNA damage around 265 nm, protein oxidation and membrane disruption in the 280-300 nm region, and oxidative stress-driven pathways between 300-350 nm. Acting in concert, these mechanisms enhance overall germicidal efficacy and minimize the survival of resistant subpopulations, thereby suppressing the tailing effect commonly observed with single-wavelength sources. [32,33] Recent literature [34-41] (summarized in Table S2, SI) reinforce this multi-wavelength advantage, showing that combined or broadband sources consistently achieve stronger reductions than single-wavelength irradiation. For example, Uppinakudru et al. [41] showed that individual LEDs at 265, 275, or 310 nm typically achieved ~3-5 log reductions, whereas operating them together produced > 7-log reduction, underscoring the role of wavelength synergy. Ma et al. [37] further confirmed this effect by demonstrating that while single exposures at 222 or 265 nm yielded only ~3-4 log reductions, sequential treatments combining UVC (222/265 nm) with UV-A (365 nm) suppressed regrowth and DNA repair, resulting in \sim 6-7 log reductions. In a similar vein, Rito et al. [35] reported achieving ~9-log reduction of E. coli through the combined use of four discrete UVC LEDs emitting at 275, 285, 300, and 340 nm. Our broadband chip therefore provides, for the first time, an integrated single platform capable of delivering these synergistic effects without the need for multiple discrete

Beyond germicidal efficacy, our UV chips incorporate practical advantages: mercury-free operation, compact design, and instant ON/OFF capability. Long-term stability testing showed robust performance, with $\sim\!40\text{--}45~\%$ radiant flux attenuation after $\sim\!2000~\text{h}$ (Figure S2, SI), while thermal testing across $-20~^\circ\text{C}$ to 80 $^\circ\text{C}$ (Figure S1, SI) demonstrated consistent output and strong environmental tolerance. Collectively, these results highlight that our UV chips combine outstanding disinfection efficiency (9-log, 99.9999999 % reduction) with durability, thermal stability, and design practicality, making them an ideal nextgeneration solution for diverse disinfection applications, particularly in space-constrained or high-reliability settings.

4. Conclusions

This study demonstrates a 9-log reduction in *Escherichia coli* using a chip-scale, free-electron driven, mercury-free, broad-spectrum UV light source. This high performance results from a highly engineered spectral

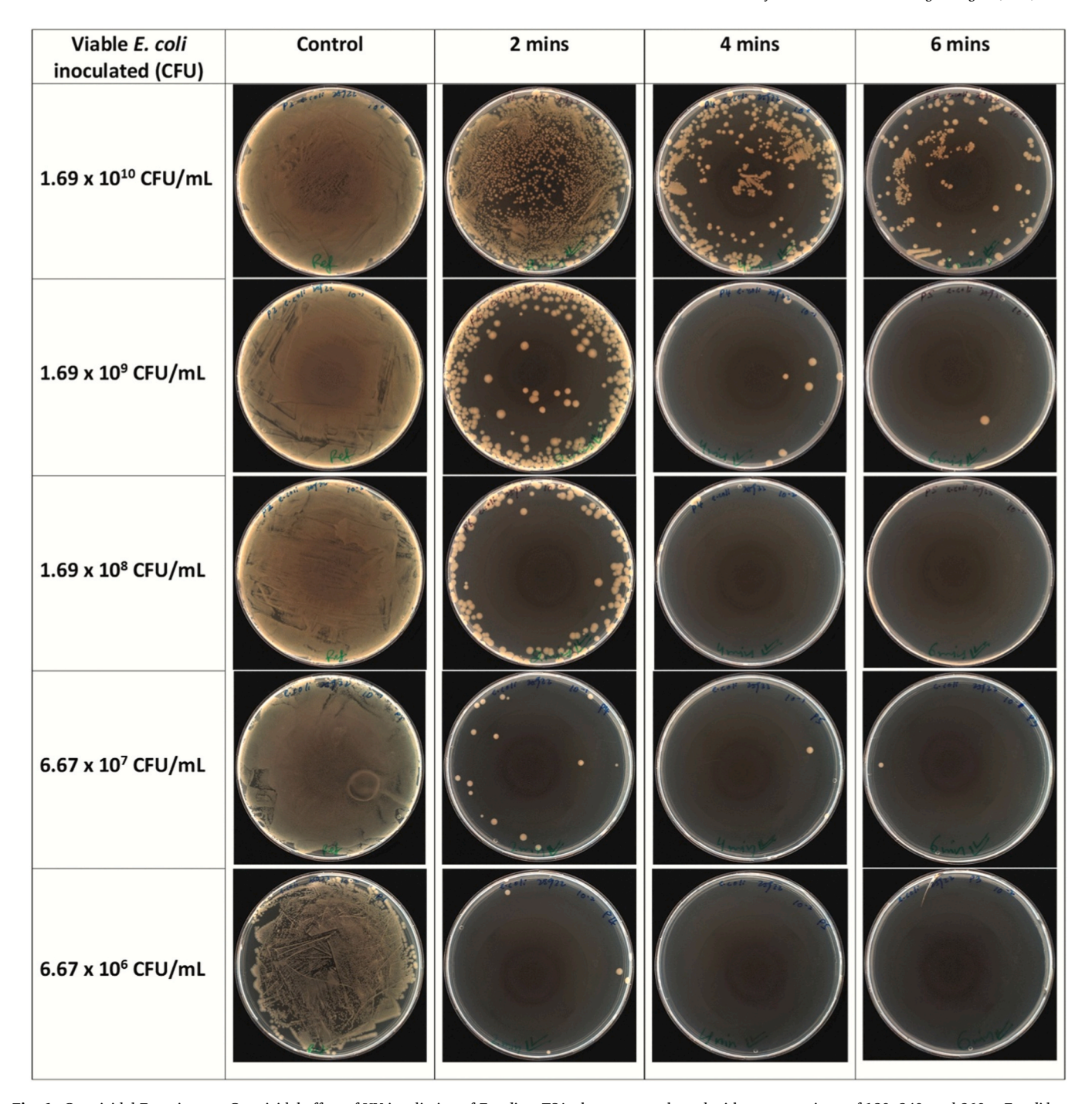


Fig. 6. Germicidal Experiments: Germicidal effect of UV irradiation of *E. coli* on TSA plates was evaluated with exposure times of 120, 240, and 360 s. *E. coli* lawns were prepared from dilutions ranging from log 6–10 CFU/mL. Controls were not exposed to UV irradiation but were otherwise treated identically to irradiated plates.

output that delivers a 70 % overlap with the *E. coli* deactivation curve and have abroad UV emission 250–350 nm This broadband emission enables simultaneous activation of multiple germicidal pathways—direct DNA damage near 265 nm, protein oxidation and membrane disruption in the 280–300 nm region, and oxidative stress—driven mechanisms between 300–350 nm—thereby maximizing disinfection efficacy through synergistic interactions of UVC-induced DNA damage and UVB-enhanced oxidative stress. The device operates efficiently at a dose of $\sim\!45$ mJ/cm² and outperforms conventional mercury-based lamps and narrow-spectrum UVC LEDs in both effectiveness and practical deployment.

With no requirement for thermal management, cold emission operation, and broad surface coverage, this solid-state UV platform offers

scalability, safety, and integration potential across a wide range of disinfection applications. From food processing lines to hospitals and household appliances, the technology provides a high-impact, energy-efficient solution to microbial contamination challenges.

It marks a pivotal step toward replacing legacy mercury technologies and advancing the development of compact, sustainable, and high-performance tools for infection control, surface sterilization, and bio-film prevention across critical sectors.

CRediT authorship contribution statement

Vijay Kumar Sharma: Writing – review & editing, Writing – original draft, Validation, Methodology, Investigation, Formal analysis,

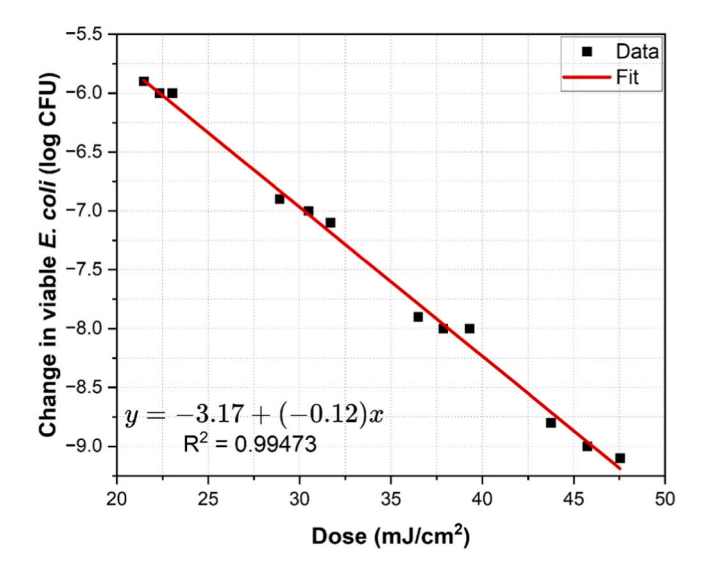


Fig. 7. Germicidal Reduction: Effect of dose of irradiation in viable cell count of *E. coli*. Results expressed as the reduction in the Colony Forming Units (CFU).

Conceptualization. Kelyn Seow: Writing – review & editing, Validation, Methodology, Formal analysis, Data curation, Conceptualization. Patricia Conway: Writing – review & editing, Supervision, Resources, Conceptualization. Emma Eriksson: Writing – review & editing, Methodology, Investigation, Conceptualization. Jonas Tirén: Writing – review & editing, Supervision, Conceptualization. Hilmi Volkan Demir: Writing – review & editing, Supervision, Project administration, Funding acquisition.

Declaration of Competing Interest

The authors declare that they have no known competing financial interests or personal relationships that could have appeared to influence the work reported in this paper.

Acknowledgements

This work is the result of a collaborative project titled "Next-Generation Ultralow-Cost High-Efficiency Eco-Friendly Lamps" between NTU Singapore and PureFize Technologies AB (previously LightLab Sweden AB).

Appendix A. Supporting information

Supplementary data associated with this article can be found in the online version at doi:10.1016/j.jece.2025.119855.

Data availability

Data will be made available on request.

References

- [1] World Health Organization, E. coli, (2018). (https://www.who.int/news-room/fact-sheets/detail/e-coli) (accessed August 14, 2024).
- [2] G. Shineh, M. Mobaraki, M.J. Perves Bappy, D.K. Mills, Biofilm formation, and related impacts on healthcare, food processing and packaging, industrial manufacturing, marine industries, and Sanitation—A review, Appl. Microbiol 3 (2023) 629–665, https://doi.org/10.3390/applmicrobiol3030044.
- [3] P. McClure, The impact of E. Coli O157 on the food industry, World J. Microbiol Biotechnol. 16 (2000) 749–755, https://doi.org/10.1023/A:1008997310966.
- [4] R. Scott, L.T. Joshi, C. McGinn, Hospital surface disinfection using ultraviolet germicidal irradiation technology: a review, Health Technol. Lett. 9 (2022) 25–33, https://doi.org/10.1049/htl2.12032.
- [5] E. Petri, M. Rodríguez, S. García, Evaluation of combined disinfection methods for reducing escherichia coli O157:H7 population on Fresh-Cut vegetables, Int J.

- Environ. Res Public Health 12 (2015) 8678–8690, https://doi.org/10.3390/
- [6] H. Wang, L. Zhang, H. Luo, X. Wang, J. Tie, Z. Ren, Sterilizing processes and mechanisms for treatment of escherichia coli with Dielectric-Barrier discharge plasma, Appl. Environ. Microbiol 86 (2019), https://doi.org/10.1128/AEM.01907-10
- [7] S. Paraskevopoulos, P. Smeets, Quantifying the log reduction of pathogenic microorganisms by constructed wetlands: a review, in: The 4th International Electronic Conference on Water Sciences, MDPI, Basel Switzerland, 2019, p. 9, https://doi.org/10.3390/ECWS-4-06433.
- [8] S.S. Basak, A. Adak, Physicochemical methods for disinfection of contaminated surfaces – a way to control infectious diseases, J. Environ. Health Sci. Eng. 22 (2024) 53–64, https://doi.org/10.1007/s40201-024-00893-2.
- [9] P. Guo, D. Luo, Y. Wu, S. He, J. Deng, H. Yao, W. Sun, J. Zhang, Coverage planning for UVC irradiation: robot surface disinfection based on swarm intelligence algorithm, Sensors 24 (2024) 3418, https://doi.org/10.3390/s24113418.
- [10] V.K. Sharma, H.V. Demir, Bright future of Deep-Ultraviolet photonics: emerging UVC Chip-Scale Light-Source technology platforms, benchmarking, challenges, and outlook for UV disinfection, ACS Photonics 9 (2022) 1513–1521, https://doi.org/ 10.1021/acsphotonics.2c00041.
- [11] A.S. Rufyikiri, R. Martinez, P.W. Addo, B.-S. Wu, M. Yousefi, D. Malo, V. Orsat, S. M. Vidal, J.H. Fritz, S. MacPherson, M. Lefsrud, Germicidal efficacy of continuous and pulsed ultraviolet-C radiation on pathogen models and SARS-CoV-2, Photochem. Photobiol. Sci. 23 (2024) 339–354, https://doi.org/10.1007/s43630-023-00521-2.
- [12] B.-M. Song, G.-H. Lee, H.-J. Han, J.-H. Yang, E.-G. Lee, H. Gu, H.-K. Park, K. Ryu, J. Kim, S.-M. Kang, D. Tark, Ultraviolet-C light at 222 nm has a high disinfecting spectrum in environments contaminated by infectious pathogens, including SARS-CoV-2, PLoS One 18 (2023) e0294427, https://doi.org/10.1371/journal.pone.0294427.
- [13] M. Perluigi, F. Di Domenico, C. Blarzino, C. Foppoli, C. Cini, A. Giorgi, C. Grillo, F. De Marco, D.A. Butterfield, M.E. Schininà, R. Coccia, Effects of UVB-induced oxidative stress on protein expression and specific protein oxidation in normal human epithelial keratinocytes: a proteomic approach, Proteome Sci. 8 (2010) 13, https://doi.org/10.1186/1477-5956-8-13.
- [14] United Nations Environment Programme, Minamata Convention on Mercury, 2019. (https://minamataconvention.org/) (accessed August 13, 2024).
- [15] Advanced UV for Life Association, UV Zero Mercury Countdown, (2024). (htt ps://lightspeed.advanced-uv.de/uv-zero-mercury-countdown/) (accessed August 19, 2024).
- [16] Z. Chen, S. Deng, M. Li, M. Su, X. Zhu, Y. Wang, Z. Chen, J. Deng, L. Wang, W. Sun, Carrier distribution characteristics of AlGaN-based ultraviolet light-emitting diodes at elevated temperatures, Journal Materials Science Materials Electronics 33 (2022) 17395–17403, https://doi.org/10.1007/s10854-022-08621-y.
- [17] J. Chen, S. Loeb, J.-H. Kim, LED revolution: fundamentals and prospects for UV disinfection applications, Environ. Sci. (Camb. 3 (2017) 188–202, https://doi.org/ 10.1039/C6EW00241B.
- [18] C. Zhang, K. Jiang, X. Sun, D. Li, Recent progress on AlGaN based deep ultraviolet Light-Emitting diodes below 250 nm, Cryst. (Basel) 12 (2022) 1812, https://doi. org/10.3390/cryst12121812.
- [19] K.D. Rauch, S.A. MacIsaac, B. Reid, T.J. Mullin, A.J. Atkinson, A.L. Pimentel, A. K. Stoddart, K.G. Linden, G.A. Gagnon, A critical review of ultra-violet light emitting diodes as a one water disinfection technology, Water Res X 25 (2024) 100271, https://doi.org/10.1016/j.wroa.2024.100271.
- [20] I. Mazumder, K. Sapra, A. Chauhan, M. Mathew, K. Singh, A review of state of the art fabrication approaches for efficiency improvement in ultra-violet region light emitting diodes, Mater. Sci. Semicond. Process 189 (2025) 109270, https://doi. org/10.1016/i.mssp.2025.109270.
- [21] R. Ishii, A. Yoshikawa, K. Nagase, M. Funato, Y. Kawakami, Temperature-dependent electroluminescence study on 265-nm AlGaN-based deep-ultraviolet light-emitting diodes grown on AlN substrates, AIP Adv. 10 (2020), https://doi.org/10.1063/5.0024179
- [22] V. Jmerik, V. Kozlovsky, X. Wang, Electron-Beam-Pumped UVC emitters based on an (Al,Ga)N material system, Nanomaterials 13 (2023) 2080, https://doi.org/
- [23] Y. Chen, Z. Zhang, H. Jiang, Z. Li, G. Miao, H. Song, L. Hu, T. Guo, Realization of an efficient electron source by ultraviolet-light-assisted field emission from a onedimensional ZnO nanorods/n-GaN heterostructure photoconductive detector, Nanoscale 11 (2019) 1351–1359, https://doi.org/10.1039/C8NR08154A.
- [24] V.K. Sharma, S.T. Tan, Z. Haiyang, S. Shendre, A. Baum, F. Chalvet, J. Tirén, H. V. Demir, On-Chip Mercury-Free Deep-UV Light-Emitting sources with ultrahigh germicidal efficiency, Adv. Opt. Mater. 9 (2021), https://doi.org/10.1002/ adva.2021.0021
- [25] R. Sommer, M. Lhotsky, T. Haider, A. Cabaj, UV Inactivation, Liquid-Holding Recovery, and Photoreactivation of Escherichia coli O157 and Other Pathogenic Escherichia coli Strains in Water, 2000.
- [26] N. Jubair, M. R, A. Fatima, Y.K. Mahdi, N.H. Abdullah, Evaluation of catechin synergistic and antibacterial efficacy on biofilm formation and acra gene expression of uropathogenic E. Coli clinical isolates, Antibiotics 11 (2022) 1223, https://doi.org/10.3390/antibiotics11091223.
- [27] A. Verónica Carabias, M.I. Gil, J.M. Pérez, M. Abellán, A. Rancaño, P. José Simón, P. Truchado, A. Allende, Fluence requirements in existing UV disinfection facilities to comply with EU validation performance targets for reclaimed water: a case study, Water Sci. Technol. 88 (2023) 1131–1141, https://doi.org/10.2166/ wst 2023 258

- [28] W.A.M. Hijnen, A.J. van der Veer, E.F. Beerendonk, G.J. Medema, Increased resistance of environmental anaerobic spores to inactivation by UV, Water Supply 4 (2004) 55–61, https://doi.org/10.2166/ws.2004.0028.
- [29] A.S. Rufyikiri, R. Martinez, P.W. Addo, B.Sen Wu, M. Yousefi, D. Malo, V. Orsat, S. M. Vidal, J.H. Fritz, S. MacPherson, M. Lefsrud, Germicidal efficacy of continuous and pulsed ultraviolet-C radiation on pathogen models and SARS-CoV-2, Photochem. Photobiol. Sci. 23 (2024) 339–354, https://doi.org/10.1007/s43630-023-00521-2.
- [30] E. Petri, M. Rodríguez, S. García, Evaluation of combined disinfection methods for reducing escherichia coli O157:H7 population on fresh-cut vegetables, Int J. Environ. Res Public Health 12 (2015) 8678–8690, https://doi.org/10.3390/ ijerph120808678.
- [31] T. Hayashi, K. Oguma, Y. Fujimura, R.A. Furuta, M. Tanaka, M. Masaki, Y. Shinbata, T. Kimura, Y. Tani, F. Hirayama, Y. Takihara, K. Takahashi, UV lightemitting diode (UV-LED) at 265 nm as a potential light source for disinfecting human platelet concentrates, PLoS One 16 (2021) e0251650, https://doi.org/ 10.1371/journal.pone.0251650.
- [32] M.J. Mattle, T. Kohn, Inactivation and tailing during UV 254 disinfection of viruses: contributions of viral aggregation, light shielding within viral aggregates, and recombination, Environ. Sci. Technol. 46 (2012) 10022–10030, https://doi.org/10.1021/es302058v
- [33] E. Vitzilaiou, A.M. Kuria, H. Siegumfeldt, M.A. Rasmussen, S. Knøchel, The impact of bacterial cell aggregation on UV inactivation kinetics, Water Res 204 (2021) 117593, https://doi.org/10.1016/j.watres.2021.117593.
- [34] Z. Jing, Z. Lu, D. Santoro, Z. Zhao, Y. Huang, Y. Ke, X. Wang, W. Sun, Which UV wavelength is the most effective for chlorine-resistant bacteria in terms of the

- impact of activity, cell membrane and DNA? Chem. Eng. J. 447 (2022) https://doi.org/10.1016/j.cej.2022.137584.
- [35] B. Rito, L. Matos, D.N. Proença, P.V. Morais, Kinetics of inactivation of bacteria responsible for infections in hospitals using UV-LED, Heliyon 10 (2024), https://doi.org/10.1016/j.heliyon.2024.e30738.
- [36] Q. Liu, X. Wang, L. Jiang, Y. Fan, F. Gao, Y. Wu, L. Xiong, Disinfection efficacy and safety of 222-nm ultraviolet c compared with 254-nm ultraviolet C: systematic review and meta-analysis, J. Hosp. Infect. 161 (2025) 55–67, https://doi.org/ 10.1016/j.jhin.2025.04.004.
- [37] D. Ma, N.M. Hull, Impact of wavelength, exposure sequence, and organic matter on UV disinfection and DNA repair, PLOS Water 4 (2025), https://doi.org/10.1371/ journal.pwat.0000306
- [38] P.O. Nyangaresi, T. Rathnayake, S.E. Beck, Evaluation of disinfection efficacy of single UV-C, and UV-A followed by UV-C LED irradiation on escherichia coli, B. Spizizenii and MS2 bacteriophage, in water, Sci. Total Environ. 859 (2023) 160256, https://doi.org/10.1016/j.scitotenv.2022.160256.
- [39] S. Probst-Riid, P.O. Nyangaresi, A.A. Adeyeye, M. Ackermann, S.E. Beck, K. McNeill, Synergistic effect of UV-A and UV-C light is traced to UV-induced damage of the transfer RNA, Water Res 252 (2024), https://doi.org/10.1016/j. watres.2024.121189.
- [40] K. Song, F. Taghipour, M. Mohseni, Microorganisms inactivation by wavelength combinations of ultraviolet light-emitting diodes (UV-LEDs), Sci. Total Environ. 665 (2019) 1103–1110, https://doi.org/10.1016/j.scitotenv.2019.02.041.
- [41] A.P. Uppinakudru, M. Martín-Sómer, K. Reynolds, S. Stanley, L.F. Bautista, C. Pablos, J. Marugán, Wavelength synergistic effects in continuous flow-through water disinfection systems, Water Res X 21 (2023), https://doi.org/10.1016/j. wroa.2023.100208.